

Evaluation of Nitrogen Oxides pollution in industrial area, Mdhilla (mining basin of Gafsa, south-western of Tunisia) with aid of GIS

Raja Mohamed, Dalila Taieb, Ammar Ben Brahim*

Research Unit: Applied Thermodynamics (UR 11 ES 80), National Engineering School of Gabes, Omar Ibn El Khattab Street 6029 Gabès, Gabès University, Tunisia.

**Corresponding Author: raja.raja200999@yahoo.com*

Tel: +21696633980, Fax: +216 76210466

Abstract

Gaseous emissions of pollutants from industries are responsible for rising discomfort and increasing airway way diseases. To prevent harmful environmental effects there is a widespread interest in controlling and regulating gaseous emissions, but sources of contaminations are often difficult to monitor. To satisfy the above-mentioned needs, the generally accepted suggestion presented in this work is to use a geographic information system (GIS) as a management tool for air pollution control.

This study aims primarily to present statistical analysis and cartography of Nitrogen Oxides in industrial areas (Mdhilla, near a factory of transformation of rough phosphate into super triple phosphate) using a geostatistical method, simple and ordinary kriging were selected for this study. It further investigates the chemical composition of rain water samples in Mdhilla. All samples were analyzed for major anions (Cl^- , SO_4^{2-} , NO_3^-) by (Shimadzu Degasser SCL.10ASP) ion chromatography instrument ,and and F^- by the potentiometric method. Major cations (Na^+ , K^+ , Mg^{2+} , Ca^{2+}) were measured by Atomic spectrometer spectra AA 220 FS. Statistical analysis was performed to identify the relationship among elements in samples of water and their possible sources.

The study includes determination of NO_3^- in dust around the industrial area (Mdhilla).

Hourly passive samples collected in 18 sample points (A1, A2, A3, A4, A5, A6, B1, B2, B3, B4, B5, B6, C1 C2, C3, C4, C5, C6) in the city of Mdhilla shows that NO_x concentration frequently exceeds the $200 \mu\text{g}/\text{m}^3$ World Health Organization standard limit and there is no exceeding of the $660 \mu\text{g}/\text{m}^3$ Tunisian standard limit recorded in all stations.

Rain water quality is characterized by a PH value ranging from 4, 10 to 6, 97. The results of this study suggest that rain water quality is strongly affected by atmospheric pollutants.

Keywords— GIS; Spatial Analysis; Air pollution; Statistical analysis; cartography; acid rain.

1. Introduction

Air quality is important simply because we have to breathe the air around us. The air we breathe is a mixture of gases and small solid and liquid particles. Some substances come from natural sources while others are caused by human activities such as our use of motor vehicles, domestic activities, industry and business. Air pollutants can cause a variety of health problems - including breathing problems; lung damage; bronchitis; cancer; and nervous system damage. Air pollution can also irritate the eyes, nose and throat, and reduce resistance to flu and other illnesses. Air pollution causes haze and smog, reduces visibility, dirties and damages buildings and other landmarks, and harms trees, lakes and animals. [1]

People who live in industrial cities should be especially concerned, since they are exposed to a greater amount of pollutants coming from industries, automobile traffic, as well as other sources.

One of the effects of air pollution is the formation of acid rain, recognized as a global environmental problem. [1]

The term 'acid rain' seems to have first been mentioned by the pharmacist Ducros in 1845. However, it was Robert Angus Smith (1872) who first conducted detailed studies of acid rain and described many of its potentially harmful effects in and around Manchester. [2]

Acid rain is now a worldwide environmental issue and the subject of a large and rapidly expanding scientific literature.

Acid rain occurs when sulfur dioxide (SO₂) and nitrogen oxides (NO_x) react in the atmosphere to form sulfuric and nitric acids, respectively. The air pollutants are transformed in the atmosphere to H₂SO₄ and HNO₃, transported across distances potentially as far as hundreds of

kilometers, and deposited as precipitation (wet deposition) and as gas and particles(dry deposition) .[3]

Keeping the air quality acceptable has become an important task for decision makers as well as for non-governmental organizations. Particulate matter and gaseous emissions of pollutant emission from industries and auto exhausts are responsible for rising discomfort, increasing airway diseases and deterioration of artistic and cultural patrimony in urban centres .[3]

Spatial interpolation is common practice in a variety of studies, especially those involving environmental variables. Essentially, the goal of interpolation is to discern the spatial patterns of a phenomenon by estimating predicting values at unsampled locations based on measurements at sample points. When concerning air pollution, the result is a surface (map) of air pollution concentrations. These maps are typically produced to visualize the spatial distribution of air pollution levels and to estimate human and vegetation exposure to pollution. [4]

Some models used in this study are integrated in a GIS, which is able to utilize the spatial information and describe the distribution of the pollutants in the atmosphere.

There are numerous definitions of GIS. A widely accepted definitions is the one given by Buvrough and McDonnel (1998) who defines it as a powerful set of tools for collecting, storing, retrieving, transforming and displaying spatial data from the real world for a particular set of purposes. [5]

Since 1990, GIS has become a common tool in environmental monitoring due to its low cost and user-friendly interface.

Nowadays, the applications of GIS are innumerable; it helps turn environmental science into policy by using relevant geographically located information and combining it with algorithm procedures [6]. GIS helps to detect and map spatial and temporal trends, assess and localize environmental risk, integrate, analyze, synthesize and display site-specific measurement data,

digital maps and metadata [7]. This system permits the simulation of spatial and temporal data of the main pollutant [8]. The principal value of using a GIS is that it enables any mathematical model to be applied with as many variables as necessary [9]. In this paper statistical and geo-statistical techniques were used to estimate NO_x concentration. After analysing data and obtaining a good variogram, cartography was used to estimate NO_x concentration at unsampled point.

2. The Study area

2.1. Geology

Gafsa is the capital of Gafsa Governorate of Tunisia. It lies 369Km by road southwest of Tunis. The geographical coordinates of the city are $34^{\circ}25'N8^{\circ}47'E$. It is located in one perforated in the middle of an alignment mountainous, called “mounts of Gafsa “ between DjbelBou-Ramli and DjbelOrbata which culminates to 1165 meters.

The governorate of Gafsa is composed of different towns such as: El Guettar, El Kaser, Gafsa, Mdhila, Mévlaoui, Moularès, Rdyef and Sned. The city has 90.000 inhabitants (2005 estimate), the governorate has 340.000 inhabitants (2005 estimate) and an area of 8990Km². (see fig 1)

The mining basin of Gafsa is a part of the south-western dry area of Tunisia. It covers 325Km², representing 42% of the entire governorate of Gafsa area and 38% of its total population [10].

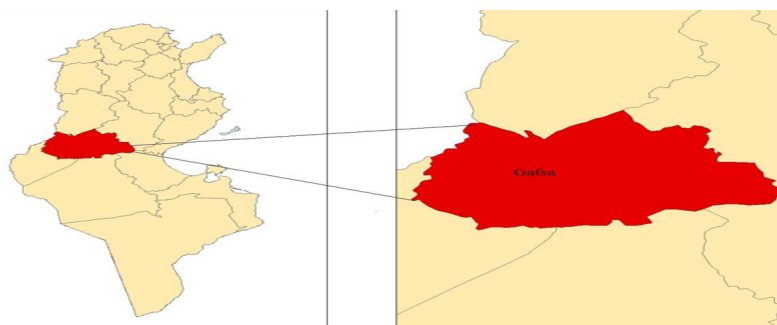


Fig.1. Study area

2.2. Soil type

The Soil in Gafsa is characterized by high salinity. It is stony and contains gypseous crusts and limestone. Mobility of sand is the limiting factor for the development of soil and rain-fed agriculture in general [11].

2.3. Vegetation

Vegetation includes steppe of this climate; *Thymeleahirusta* (menten), *Artemisia eampestris* (tgouft), *Artemisia bleached on grass Alba* (chir), *Diplotaxix* (harra) and *Peganumharmala* (harmel). The Oasis of south –western Gafsa El-Kasba, El ksar, Lala and Guettar covers about 3200 hectares. The oasis counts 32500 palm trees belonging to seven different variets; “Degletnour”, “Allique “, “Kenta”, “BesserHlou”, “Quabrichou” and “Hammouri”[12].

2.4. Metrological condition

2.4.1. Rain

The annual precipitation of the city is always lower than 200mm. The wet season extends from September to April while the dry season lasts from May to October. July to August is the driest and warmest period. The monthly rainfall between 1981 and 2005 (see table 1) [13].

Table1. Monthly rainfalls between 1981 and 2005

Months	September	October	November	December	January	February	March	April	May	june	julay	August
monthly average	7,2	16,3	19,3	16,9	24,8	11,1	15,9	5	14,7	6,5	3,9	6,7

2.4.2. Wind

Winds play a significant role in the transport and dilution of pollutants. Pollutant dispersion is also significantly affected by variability in wind direction .If wind direction is relatively constant the same area will be continuously exposed to high pollutants levels .If, on the other hand, wind direction is constantly shifting, pollutants will be dispersed over a larger area and concentrations over any given exposed area are lower .

Wind speed varied from 1m/s to ≥ 16 m/s in the period between 2007 and 2011 and winds were predominately from northeast. Wind direction frequency and wind speed for a given time period may be summarized by constructing a wind rose (fig 2) and (table 2) [14].

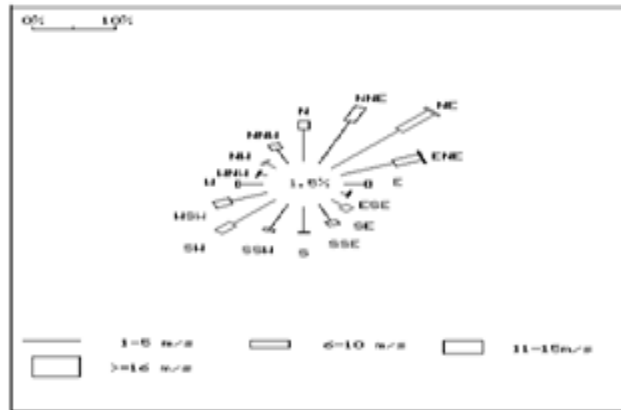


Fig.2. Wind rose (between 2007 and 2011)

Table2.Frequency of wind (2007-2011)

direction /	1-5 m/S	6-10	11-15	>=16 m/s	total
N	6.8	1.7	0.1	+	8.6
NNE	9.7	3.3	0.1	+	13.1
NE	11.4	5.6	0.2	+	17.2
ENE	6.8	3.4	0.2	0.0	10.4
E	2.6	0.5	+	0.0	3.2
ESE	0.8	0.2	0.0	0.0	1.0
SE	1.7	1.0	+	0.0	2.7
SSE	3.6	0.9	0.0	0.0	4.5
S	5.4	0.2	+	0.0	5.6
SSW	5.6	0.4	0.0	+	6.0
SW	7.0	2.4	+	0.0	9.4
WSW	4.4	2.1	0.1	0.0	6.6
W	2.8	0.4	+	+	3.2
WNW	0.8	0.2	+	0.0	1.0
NW	1.3	0.4	+	0.0	1.7
NNW	3.2	1.0	+	0.0	4.3
Total	73.9	23.7	0.9	0.0	98.5

+ indicates a non-zero frequency but <0.05%)

2.4.3. Temperature

Gafsa has a dry continental climate. It is characterized by important annual variation in temperature. The average monthly temperature varies between 9,7°C to 30, 9°C, with the highest peak in July (fig 3) [15].

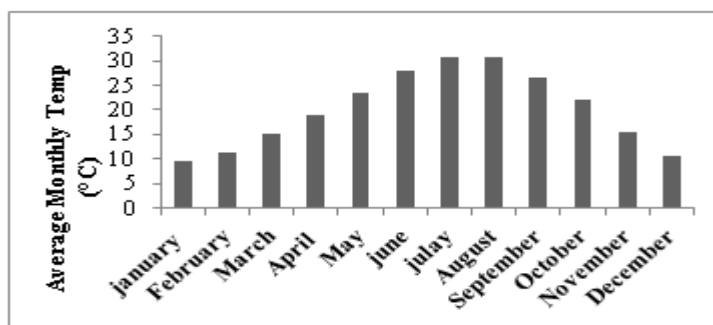


Fig.3. Average Monthly Temperature (°C)

2.5. Industry

Gafsa also specializes in the Craft industry of wool carpets, in particular the Klim and the Margoum which are intended for exportation.

Gafsa is also considered as one of the most important phosphate areas in the world. Its phosphate layer was discovered in 1886. In 2005, eight million tons were extracted from its mines; which make Tunisia the fifth world producer [16]. (See table 3).

Table 3. Rank of Tunisia in level of production of phosphate

Pays	Production(106k)	World share (%)
Etat unis	36300	24.69
Chine	30400	20.68
Maroc	25200	17.14
Russie	11000	7.48
Tunisie	8000	5.44

3. Materials and methods

3.1. Sampling Sites

3.1.1 Nitrogen oxide NO_x in ambient air in Mdhilla

Data were collected at 18 locations (sample point) in the city of Mdhilla (table 4) and (fig 4).

Mdhilla is located at approximately 18 Km of the town of Gafsa in the south-west of Tunisia. The source of pollution is the factory located at 4Km outside Mdhilla. The principal activity of this factory is the transformation of rough phosphate into super triple phosphates. The transformational sequence is carried out in three stages starting from the combustion of Sulphur to produce Sulphuric acid; to the production of the TSP that is made from phosphate and finally to the production of the phosphoric acid [17].

Table 4. Location of passive monitoring

Points	Coordinates (Labo)	
	UTM(32)	
	X	Y
A1	3794425	475549
A2	3793032	476312
A3	3793378	478758
A4	3796579	482057
A5	3800249	481601
A6	3802425	481643
B1	3795208	477043
B2	3794793	477839
B3	3794378	478448
B4	3796416	480890
B5	3798184	481418
B6	3801311	481436
C1	3795632	477797
C2	3795207	478307
C3	3795047	478766

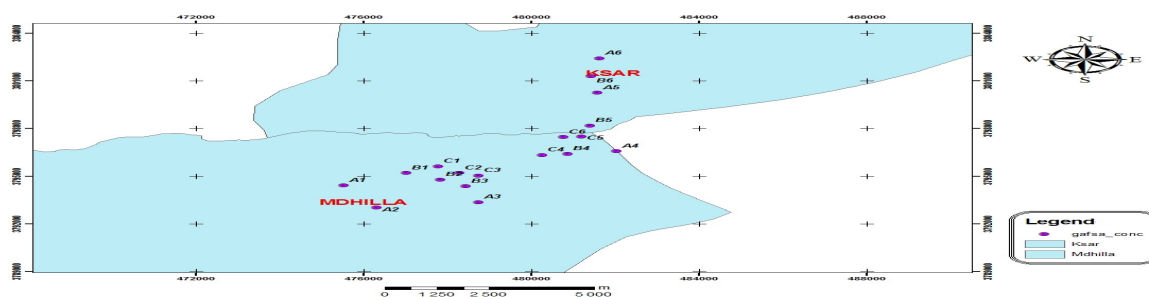


Fig.4. Sampling Site

3.1.2. Dust

A total of 3 samples were collected using air blower (Black and Decker, serial number (49613) in the city of Mdhilla (fig 5). These samples were collected during January 2011.

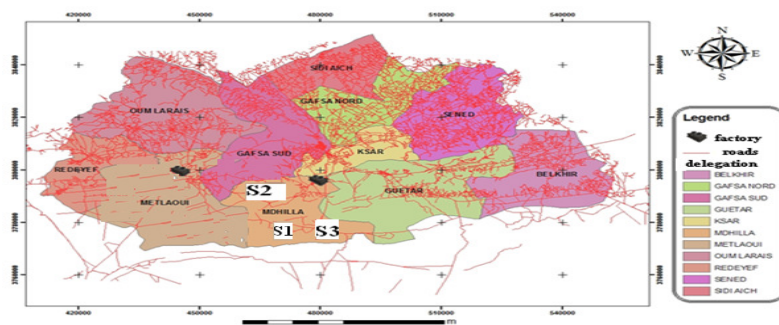


Fig.5. Location of Sampling Sites.

3.1.3. Rain

Rain samples were collected in the city of Mdhilla near Landry of phosphate. The 3 samples were collected over a 24- hour period. Details of sampling are given in (table 5).

Table 5. Sampling collection

Station code	Period sampling
E1	8 AM-11AM
E2	11AM-14 PM
E3	14PM-17PM

3.2. Passive diffusion tubes

Passive sampling is a practical and cost-effective technique for assessing air quality in different environments over relatively long exposure periods (usually from 1 day to 5weeks) depending on the design of the device [18].

The concentration is classically determined from the collected amount of analyte divided by the sampling time and the sampling rate by applying Fick’s first law [19].

Passive samplers, either diffusive or permeative, are in principle formed as tubes or boxes which are performed in order to improve efficiency, reduce sensitivity to air fluctuations and simplification of analyte desorption [20]. Passive samplers are generally protected from the rain, sun and chemical damage during field deployment by a shelter of various designs [21].

At each sample point concentration was measured with diffusion tubes.

3.3 .Statistical analysis

To identify the relationship among elements in the water samples and their possible sources, Pearson's correlation coefficient analysis, principal component analysis (PCA) and cluster analysis (CA) were performed.

3.3.1. Pearson's correlation coefficient analysis

The Pearson correlation coefficient measures the strength of relationships between pairs of contaminants within samples.

3.3.2. cluster analysis (CA)

Hierarchical cluster analysis (HCA) comprises an unsupervised classification procedure that involves measuring either the distance or the similarity between objects to be clustered.

The resulting structure is a sequence of nested partitions which can be visualized using a graphic called Dendogram (Tree) in which the nodes represent clusters of the first analyzed set .In particular, the initial set is the root of the tree while the leaves represent the singletons.

The hierarchical CA was performed using the following settings: The linkage type used was Ward's method and the distance method was Euclidean distances. [22]

3.3.3. Principal component analysis (PCA)

The central idea of principal component analysis (PCA) is to reduce the dimensionality of a data set consisting of a large number of interrelated variables, while retaining as much as possible the variation present in the data set. [23]

PCA has been broadly used as an exploratory tool to identify the major sources of pollutant emission and to statistically select independent source tracers. In mathematical terms, PCA relies upon an eigenvector decomposition of the covariance or correlation matrix. [24].

We performed the PCA with a varimax rotation and retention of principal components whose eigenvalues were greater than unity by adopting Kaiser's criteria. Each variable in a

factor is used to identify the correlation between each component, the pollutant and emission source [25].

3.4. Geostatistical techniques

Three phases were completed to conduct the geostatistical work:

(1) Exploratory analysis of data: Data were studied without considering their geographical distribution. Statistics were applied to check data consistency, removing outliers and identifying statistical distribution.

(2) Structural analysis of data: Spatial distribution of the variable was analysed. Spatial correlation or dependence can be quantified with semivariograms, or simply variograms.

3) Predictions: The main objective of a geostatistical study is to obtain estimates of values of the studied variable at unsampled locations, considering the spatial distribution pattern and integrating information from sample points.

The geostatistical analyses were carried out with the extension Geostatistical Analyst of the GIS software ArcGIS (version 9.3).

Maps of kriged estimates provided a visual representation of the distribution of the atmospheric pollution in Gafsa. These maps were produced with ArcMap module of the ArcGIS, after conducting the geo-statistical study

3.5. Chemical Analysis

All samples of rain and dust were analyzed for major anions (SO_4^{2-} , Cl^- , NO_3^-) by (Shimadzu Degasser SCL.10ASP) ion chromatography instrument. F^- by a potentiometric method. Major cations (Na^+ , K^+ , Mg^{2+} and Ca^{2+}) were measured by Atomic spectrometer spectra AA 220 FS. The pH values of the collected samples were measured using pH meter equipped with a combination of glass electrodes. Calibration was always carried out before measurement using standards buffer solutions

4. Results and discussion

4.1 Level of Nitrogen oxide NOx in ambient air in Mdhilla

4.1. 1.Statistical Analysis of Nitrogen oxide NOx

Looking at the graph and table (6) above, there is no point that exceeds the Tunisian standard limit ($660\mu\text{g}/\text{m}^3$) during the passive monitoring period. But NOx concentration frequently exceeds the $200\mu\text{g}/\text{m}^3$ World Health Organization standard limit.

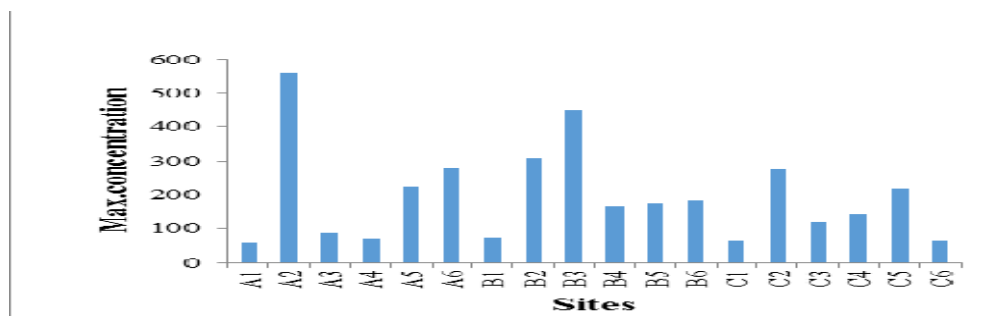


Fig.6.Hourly Max concentration NOx (µgm3)

Table 6.Concentrations of NOx

Points	Max. Hourly Concentration. NOx
	(µg/m3)
A1	57.64
A2	556.34
A3	88.55
A4	68.77
A5	222.03
A6	278.07
B1	71.78
B2	307.74
B3	450.3
B4	165.8
B5	173.88
B6	182.93
C1	63.26
C2	275.99
C3	117.27
C4	143.78
C5	217.81
C6	64.72

4.1.2. Cartography

In this section, we establish the cartography of NO_x concentration. We use the kriging interpolation method, which is a well known spatial estimation technique developed by Krige. It takes into account the spatial structure of the studied variables describing the spatial phenomenon; the interpolation at any point is obtained using an estimator. The latter is built by linearly combining the measured values with different weights. To calculate these weights, the estimator is assumed to be a minimum. Moreover; knowledge of the variance enables us to quantify the error, intrinsic to the interpolation method, between the estimated value and the true value.

Ordinary Kriging is the most frequent implementation of kriging. A by-product of ordinary kriging is the "geo-mean", function of the variogram, which estimates the average of the data points with filtering of their spatial redundancy. It is a weighted average, giving to each data point a weight proportional to its influence in the knowledge of the field. It is the unbiased version of the statistical average. It is also the trend or drift (a constant value) to which the estimate is attracted away from the data points. The general form of kriging equation is:

$$Z(s_o) = \sum_{i=1}^N \lambda_i Z(s_i)$$

Where:

- $Z(s_o)$ is the estimated value of variable Z at point x .
- λ_i is the kriging weight for the point I .
- $Z(s_i)$ is the main variable under consideration when several are in use.
- n is the number of data points where Z is known.

4.1.3. Variogram

Before kriging, and spatial correlation or dependence data was quantified with semivariograms, and the covariance (see fig 7).

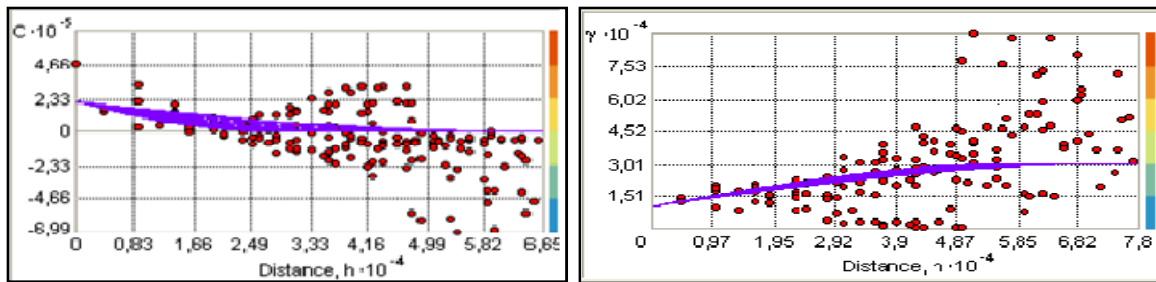


Fig.7.Spatial correlation

4.1.4. The concentration and Trend of Nitrogen oxide NO_x

Cartography (fig 8, fig 9) shows the level of NO_x at three monitoring sites (Mdhilla, Ksar and Gutar). It has been observed that there is a decreasing trend of concentration of NO_x at (Ksar and Gutar) but an increasing trend has been found at the Mdhilla site. There are several factors that possibly contribute to the increasing trend in Mdhilla (red area) such as its location near the factory, in addition to intense local urban traffic and climatic conditions that limit the dispersion of pollution.

The Regulatory limit or the background concentration of the Mdhilla region should be revised to better protect the people from air pollution in that region.

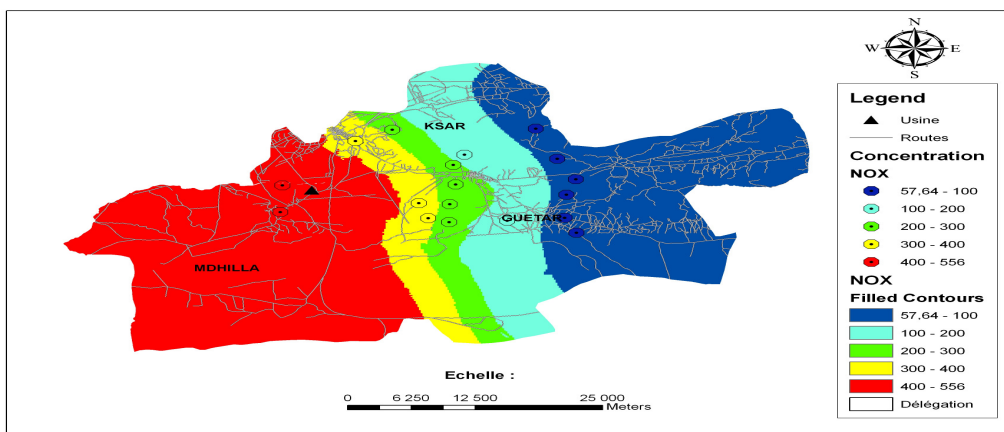


Fig.8.Simple kriging Prediction Map of NO_x.

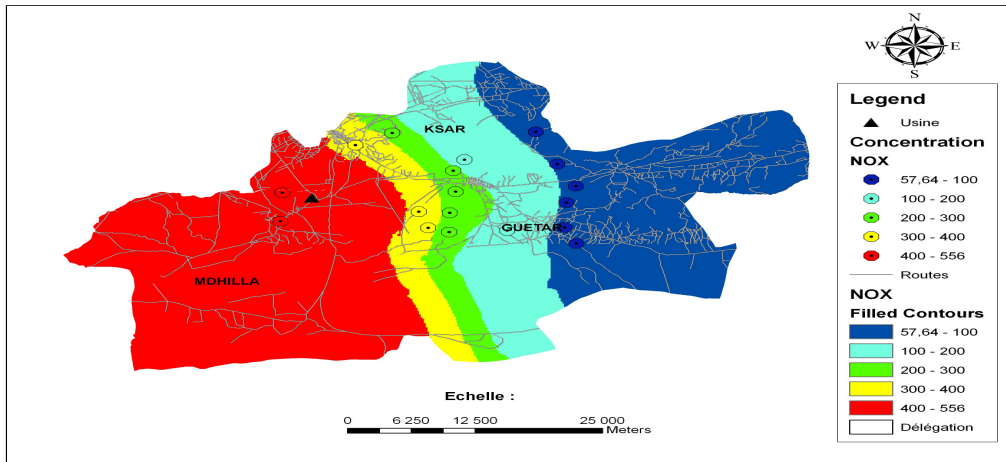


Fig.9. Ordinary kriging Prediction Map of NOx.

4.2. Nitrate (NO₃⁻) concentration in rain

Nitrate in rain water is generally attributed to the acidity of rain water

4.2.1. Chemistry of Acid Rain

4.2.1.1. PH Values

The low pH values in the rainwater samples were due to the dissolution of CO₂ and natural SO₂ source.

The relatively high pH of 6.97 measured in this study was due to the neutralization of acidity in precipitation by CaCO₃. Acidity in precipitation depends on the concentration of acid-forming ions as well as concentration of alkaline species which neutralize the acidity and the amount of rainfall as can be seen in (fig10).

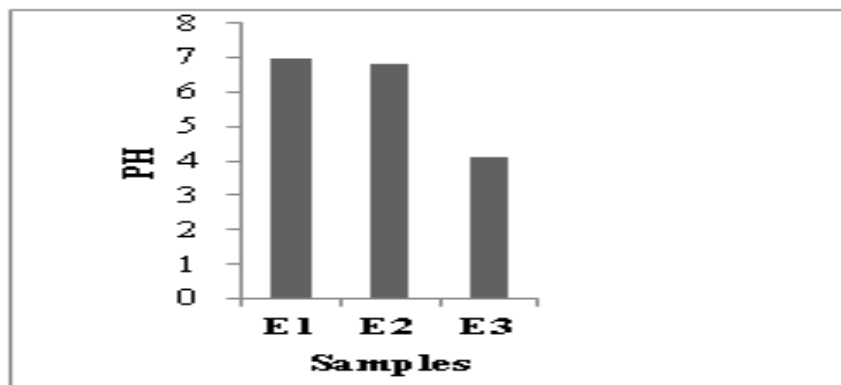


Fig.10. PH values for the different samples

4.2.1.2. Ions Concentrations

The concentration of ions in different samples is shown in (table 7) and (fig11).

All species presented wide variations from sample to sample. The sample with highest ion content is initial fraction events occurring at the beginning of the rainfall hours when large amounts of dust accumulate in the atmosphere are scavenged by rain.

The ionic abundance in precipitation showed the general trend $\text{SO}_4^{2-} > \text{Cl}^- > \text{F}^-$ for anions, and $\text{Ca}^{2+} > \text{Mg}^{2+} > \text{K}^+ > \text{Na}^+$ for cations. The SO_4^{2-} ions have the highest concentration.

Table 7. Concentrations of major ions (mg/L)

Ions /Samples	E1	E2	E3
F ⁻	1.17	1.15	0.6
SO ₄ ²⁻	48.56	15.22	11.52
Cl ⁻	6	6	0.8
Na ⁺	1.27	0.93	0.2
K ⁺	1.22	1.2	0.25
Mg ²⁺	1.34	1.22	1.22
Ca ²⁺	11	10	10
NO ₃ ⁻	27	23	17

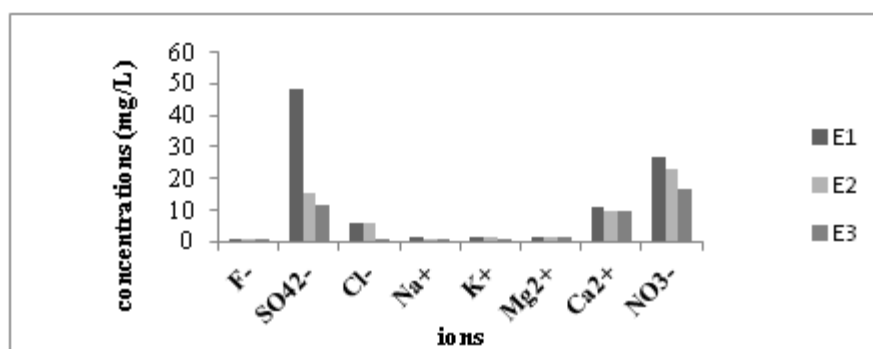


Fig.11. Ions concentrations in rain water.

4.2.1.3. SO₄²⁻/NO₃⁻

The calculated $\text{SO}_4^{2-}/\text{NO}_3^-$ ratio may indicate the anthropogenic sources in the atmospheric precipitation of industrial areas. The results obtained in this study were compared to those from other sites [25]. (table 8).

Table 8. $\text{SO}_4^{2-}/\text{NO}_3^-$ comparison ratio at various sites in the world [25]

sites	$\text{SO}_4^{2-}/\text{NO}_3^-$
E1	2.00
E2	1.00
E3	1.00
Guaiba	8.70
Figueira	5.30
Singapore	3.5
Galilee	5.37
Ankara	1.60
Spain	2.22
Italy	3.10

4.2.2. Determination of Chemical Sources

4.2.2.1. Correlation Analysis

In order to find possible relation between ions in rainwater samples, and consequently the likely sources of pollutants, correlation between ions in the rainwater was calculated and presented in (table 9).

Table shows that the Pearson correlation coefficient ions in rain water. F^- , SO_4^{2-} , Cl^- , Na^+ , K^+ , Mg^{2+} , Ca^{2+} , NO_3^- are significantly positive correlated.

F^- , SO_4^{2-} and NO_3^- are significantly positive correlated with each other at 0.05 and 0.01 level, showing similarity of their chemical behavior in rainwater and the co-emission of their precursors SO_2 , NO_x and fluoride.

Similarly, a strong correlation (1) at 0.01 level seen between Ca^{2+} and Mg^{2+} , suggesting the common source of these ions from natural source (Cristal origin).

Other relatively good correlations were observed between Ca^{2+} and SO_4^{2-} , Mg^{2+} and SO_4^{2-} , Mg^{2+} and SO_4^{2-} , K^+ and SO_4^{2-} , Ca^{2+} and NO_3^- , Mg^{2+} and NO_3^- , K^+ and NO_3^- , Ca^{2+} and F^- , Cl^- and F^- , F^- and NO_3^- , K^+ and F^- probably result from the reaction of the acids H_2SO_4 , HNO_3 , HCl and HF with alkaline compounds rich in K^+ , Mg^{2+} and Ca^{2+} carried into atmospheric environment from soil by winds. This shows that wind-carried dust and soil plays an important factor in the chemistry of rainwater.

Table9. Correlation matrix between ions in rainwater samples

	F ⁻	SO ₄ ²⁻	Cl ⁻	Na ⁺	K ⁺	Mg ²⁺	Ca ²⁺	NO ₃ ⁻
F ⁻	1.000							
SO ₄ ²⁻	0.908	1.000						
Cl ⁻	0.866	0.576	1.000					
Na ⁺	0.979	0.802	0.950	1.000				
K ⁺	0.875	0.591	1.000(*)	0.956	1.000			
Mg ²⁺	0.866	0.996	0.500	0.745	0.516	1.000	1.000(**)	
Ca ²⁺	0.866	0.996	0.500	0.745	0.516	1.000(**)	1.000	
NO ₃ ⁻	0.993	0.854	0.918	0.996	0.925	0.803	0.803	1.000

*Correlation is significant at the 0.05 level
(2-Tailed)

** Correlation is significant at the 0.01 level
(2-Tailed)

4.2.2.2. Hierarchical Cluster Analysis

Hierarchical Clustering Analysis (HCA) allows the organizations of data into an understandable framework for searching the source grouping.

The Ward's method used to obtain hierarchical associations and the Euclidean distance was used as similarity measurement.

The highest similarities are linked first, and variables connected only if they are highly correlated. After two variables are clustered, their correlations with all the other variables are averaged.

Statistical calculations were performed by using a software package SPSS version 15. The result of HCA is presented as a dendrogram (fig 12).

The Cluster has two bigger subgroups:

Group1: A first group consists of a large number of ions (Na⁺, K⁺, Mg²⁺, Ca²⁺ and Cl⁻) strongly suggests that this source is of crustal origin.

Group 2: A second group of elements consisting of F⁻, SO₄²⁻ and NO₃⁻ is strongly correlated in coefficient analysis and clearly separate from the other ions in CAH. This separation between them and other ions may suggest a mainly anthropogenic source, especially the industrial activities of factory in Mdhilla.

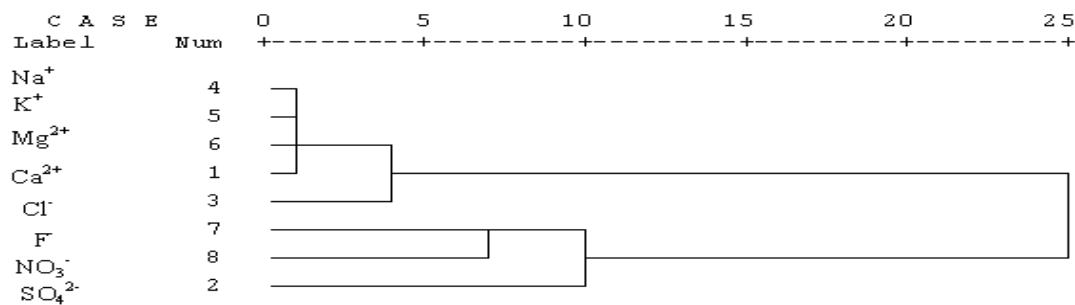


Fig.12. Dendrogram results from word method of Hierarchical cluster analysis for 8 elements.

4.3. Nitrate (NO₃⁻) concentration in dust

Nitrogen oxide (NO_x) are mostly emitted to the atmosphere as NO which is subsequently transformed into NO₂. They react with hydroxyl radicals to transform to nitric acid and nitrate by physical and chemical transformation .

It has been widely known that the nitrate in dust seems to be formed mostly by reaction between nitric acid with alkaline coarse particle such as sea-salt or dust particles in the atmosphere. [26]

The obtained results show that the NO₃⁻ concentration ranged from 1.108 to 1.227 g/ kg (Table 10).

The nitrate in dust seems to be associated with anthropogenic species because when air moves through Mdhilla it passes over the highly industrialized area. Especially the factory located at 4Km outside Mdhilla.

Table 10. Concentration of nitrate in dust (g/Kg)

sites	NO ₃ ⁻
S ₁	1.70
S ₂	1.22
S ₃	1.10

Conclusion

Results showed that GIS is an effective tool for carrying out environmental impact assessment and that the visualization and analytical features of GIS did provide more information and convenience to users

One of the outlooks of this work is to perform investigations in areas such as A5, A6, B2, B3, C2 and C5, where the NO_x concentrations may be a real concern to the population, and to environment. It would be beneficial if a close monitoring can show repeatable reproducible results in those areas.

The results showed that acid rain is one of the foremost examples of air pollution.

Acknowledgment

The authors would like to thank the administration of Biotech Pole Sidi Thabet (Tunis). Thanks are also to Mr Habib Hamid Director of Research Center, Gafsa Phosphate Company (CPG) for his help during the sampling campaigns. We are particularly indebted to Professor Marie Le Coq at laboratory of Process Engineering, Environment, Food (GEPEA) Nantes, France for her continuous and precious collaboration. Finally, we wish to express our gratitude to Thomas Bergantz for his technical support.

Reference

- [1] Na Zheng , Jingshuang Liu, Qichao Wang , Zhongzhu Liang : Heavy metals exposure of children from stairway and sidewalk dust in the smelting district, northeast of China, Atmospheric Environment ,44 (2010) 3239-3245.
- [2] E. Puliafito, M. Guevara, C. Puliafito: Characterization of urban air quality using GIS as a management system, Environmental Pollution, 122 (2003) 105–117.
- [3] A. Pederzoli ,M. Mircea , S. Finardi , A. di Sarra , G. Zanini.Quantification of Saharan dust contribution to PM10 concentrations over Italy during 2003-2005, Atmospheric Environment ,44 (2010) 4181-4190.

- [4] Fernando J. Aguilar, Fernando Carvajal, Manuel A. Aguilar, Francisco Aguera: Developing digital cartography in rural planning applications, *Computers and Electronics in Agriculture*, 55 (2007) 89–106.
- [5] Winfried Schroder: GIS, geostatistics, metadata banking, and tree-based models for data analysis and mapping in environmental monitoring and epidemiology, *International Journal of Medical Microbiology*, 296 (2006) S1, 23–36.
- [6] Arnparo Moragues, Teresa Alcaide: The use of a geographical information system to assess the effect of traffic pollution, *Environmental Pollution*, 122 (2003) 105–117.
- [7] Francis Van Jearsveld: characterising and mapping of wind transported sediment associated with opencast crypsum, March 2008.
- [8] Jialiang Feng: characteristics and source apportionment of organic matter in PM_{2.5} from cities in different climatic zones of China, January 2006, Hong Kong.
- [9] Andrew S. Goudie: Dust storms: Recent developments, *Journal of Environmental Management*, 90 (2009) 89–94.
- [10] Fatma Karaoulia, Sarra Touzib, Jamila Tarhounib, Latifa Bousselmic : Improvement potential of the integrated water resources management in the mining basin of Gafsa, *Desalination*, 246 (2009) 478–484.
- [11] Medical Force protection –Additional information :Tunisia, Threat Assessment Department Navy Environmental & Preventive Medicine Unit 2 1887 Powhatan Street Norfolk, VA 23511-3394.
- [12] Jean-Olivier Job: les sols sales de l'oasis D'el Guetar (sud tunisien), septembre 1992.
- [13] Fernando J. Aguilar, Fernando Carvajal, Manuel A. Aguilar, Francisco Aguera: Developing digital cartography in rural planning applications, *Computers and Electronics in Agriculture*, 55 (2007) 89–106.

[14] E. Puliafito, M. Guevara, C. Puliafito: Characterization of urban air quality using GIS as a management system, *Environmental Pollution*, 122 (2003) 105–117.

[15] Winfried Schroder: GIS, geostatistics, metadata banking, and tree-based models for data analysis and mapping in environmental monitoring and epidemiology, *International Journal of Medical Microbiology*, 296 (2006) S1, 23–36.

[16] Bin Han, Zhipeng Bai , HongLiang Ji, Guanghuan Guo, Fang Wang, Guoliang Shi, Xiang Li: Chemical characterizations of PM10 fraction of paved road dust in Anshan, China, *Transportation Research Part D* 14 (2009) 599–603.

[17] Raja Mohamed, Dalila Taieb, Ammar Ben Brahim, 2012. Atmospheric PM10 pollution in the mining basin of Gafsa (south-western of Tunisia): statistical analysis and cartography. *International magazine Geo SP.net*. 1-13.

[18] Fernando J. Aguilar , Fernando Carvajal, Manuel A. Aguilar, Francisco Aguera: Developing digital cartography in rural planning applications, *Computers and Electronics in Agriculture*, 55 (2007) 89–106.

[19] Sotiris Vardoulakis , Julio Lumbreras , Efisio Solazzo, 2009 . Comparative evaluation of nitrogen oxides and ozone passive diffusion tubes for exposure studies, *Atmospheric Environment*.43, 2509–2517.

[20] H. Plaisance, 2004. Response of a Palmes tube at various fluctuations of concentration in ambient air, *Atmospheric Environment*. 38, 6115–6120.

[21] Suresh Seethapathy, Tadeusz Górecki , Xiaojing Li, 2008. Passive sampling in environmental analysis. *Journal of Chromatography A*. 1184, 234–253.

[22] Jorge Pey, Xavier Querol, Andre´s Alastuey , Sergio Rodr´ıguez , Jean Philippe Putaud, Rita Van Dingenen, Source apportionment of urban fine and ultra-fine particle

number concentration in a Western Mediterranean city, *Atmospheric Environment* 43 (2009) 4407–4415.

[23] Sergiu Theodor Chelcea, *Agglomerative 2-3 Hierarchical Classification: Theoretical and Applicative Study*, thesis (2007) pp 52-56.

[24] Inoka Senaratne, David Shooter. Elemental composition in source identification of brown haze in Auckland, New Zealand. *Atmospheric Environment* 38 (2004) 3049–3059.

[25] David D. Cohen, David Garton, Ed Stelcer. Multi-elemental methods for fine particle source apportionment at the global baseline station at Cape Grim, Tasmania. *Nuclear Instruments and Methods in Physics Research, B* 161-163 (2000) 775-779.

[26] David Widory. Nitrogen isotopes: Tracers of origin and processes affecting PM₁₀ in the atmosphere of Paris. *Atmospheric Environment* 41 (2007) 2382–2390.

Figures

Fig.1. Study area

Fig.2. Wind rose (between 2007 and 2011)

Fig.3. Average Monthly Temperature (°C)

Fig.4. Sampling Sites

Fig.5. Location of Sampling Sites

Fig.6. Hourly Max concentration NO_x (µg/m³)

Fig.7. Spatial correlation

Fig.8. Simple kriging Prediction Map of NO_x

Fig.9. Ordinary kriging Prediction Map of NO_x

Fig.10. PH values for the different samples

Fig.11. Ions concentrations in rain water

Fig.12. Dendrogram results from word method of Hierarchical cluster analysis for 8 elements

